

X-ray and electron microscopical studies of thin films of $(\text{Cd}_{1-x}\text{Zn}_x)\text{S}$ solid solution

A. H. EID, S. MAHMOUD, Z. S. EL MANDOUH

Laboratory of Electron Microscopy and Thin Films, National Research Centre, Dokki, Cairo, Egypt

A series of $(\text{Cd}_{1-x}\text{Zn}_x)\text{S}$ powders phosphors and thin layers prepared by thermal evaporation of solid solution were studied. The phosphors used were 41% ZnS: 59% CdS with a cobalt concentration from 0 to 0.325%. The analysis of the structure of films of different thicknesses using X-ray diffraction technique confirms that the calculated relative intensities of the planes show considerable differences from the experimental results. For film thicknesses ~ 70 nm the a axis is normal to the substrate, while at greater thicknesses (273 nm) the c axis is practically normal to the substrate. The effect of the electron beam on the solid solution indicates that layers decomposed leaving the grain boundaries decorated by metallic cadmium and zinc particles.

1. Introduction

Some phosphors have been used as solid state dosimeters for personal dosimetry, radiobiology, radio therapy and civil defence. Solid solutions of $(\text{Cd}_{1-x}\text{Zn}_x)\text{S}$ are considered as efficient phosphors, since by varying the composition it is possible to adjust their properties, such as energy gap, crystal type and lattice parameters. Early measurements of lattice parameters of the $(\text{Cd}_{1-x}\text{Zn}_x)\text{S}$ system show large positive deviations of a and c from Vegard's law [1]. It has been suggested [2] that this deviation is attributed to the partial ionic character of the bonds which leads to an increase in the lattice energy. Domens *et al.* [3] prepared $(\text{Cd}_{1-x}\text{Zn}_x)\text{S}$ polycrystalline layers by thermal evaporation of suitable $(\text{CdZn})\text{S}$ solid solutions ($0 \leq x \leq 0.2$) on different substrates. The influence of ZnS concentration on the layer physical properties is determined by X-ray patterns, by optical spectrometry of the band gap and the free carrier absorption. When the ZnS concentration increases, the crystallization is modified, the energy gap and the activation energy of the donor levels increases. The prepared layers are homogenous ternary solid solutions with the lattice parameters c slightly lower than the crystal value, decreasing when the ZnS composition x increases. Kane *et al.* [4] confirmed that thin films of $(\text{Cd}_{1-x}\text{Zn}_x)\text{S}$ prepared by evaporation are substitutional solid solutions and solubility existed in all proportions.

When crystal of hexagonal ZnS: CdS: Ag was bombarded with high intensity cathode rays, Leverenz [5] observed skeletal striae which were probably mostly ZnS left behind by selective volatilization of CdS. In addition, daylight produces a blackening of zinc and more so of cadmium sulphide, attributed to freeing of the metal, this being a photochemical reaction. The metal becomes colloidal and the damage is irreversible [6]. The effect is marked when the quantum energy $h\nu$

is greater than the energy band gap. Morlin [7] illustrates the decomposition process as the breaking up of the single crystalline material into polycrystalline aggregates. At the same time, cavities, or larger aggregates of vacancies were produced which together with the boundaries of the polycrystalline aggregates served as nuclei for growing dark platelets which appeared to be alkali metal crystals.

The presence of a transition metal impurity such as nickel and cobalt centres in a sulphide lattice reduces the luminescent intensity [8]. They form a series of closely spaced energy levels in the forbidden band so that recombination may occur in steps with the emission of phonons or infrared radiation. Cobalt levels are located above the Fermi level and usually empty. Thus radiationless transitions of excited electrons from the conduction band to the killer levels can take place immediately after excitation.

2. Experimental technique

Studies were made on a series of ZnS: CdS: Co powder phosphors and thin layers in which the concentration of cobalt dopant varied from 0 to 0.0325%. The phosphors investigated had a host matrix ZnS: CdS ratio of 41: 59. The layers were prepared by thermal evaporation in a vacuum of $\sim 10^{-4}$ Pa using a tungsten boat and we have obtained ZnS: CdS: Co layers which were solid solutions with a composition very similar to that of the evaporated powder. The film thickness varied from 70 to 273 nm and the deposition rate at 7 nm sec^{-1} . The layers was measured by the Tolansky interference method [9]. Different substrates were used as glass slides and carbon films. The layers prepared on glass slides were examined using a Siemens D 500 X-ray diffractometer. The deposited ZnS: CdS: Co on thin carbon films were ready for the examination by transmission electron microscopy and diffraction using (Zeiss EM 10) electron microscope.

3. Results and discussion

The analysis of the structure of ZnS:CdS films of different thicknesses evaporated onto an amorphous substrate was carried out using X-ray diffraction technique in order to clarify the structure and the crystallite size of the deposited layers. X-ray diffraction patterns of considerably thick films on glass slides confirm this suggestion. As shown by Figs 1b and 1c X-ray diffraction patterns ($18 \leq 2\theta \leq 42$) reveal only the (002) orientation implying that c axis of the crystallites are practically normal to the substrate. Our results are particularly similar to the Domen *et al.* [3] result. For film thickness (70 nm) the predominant (hkl) plane is (100) indicating that the a axis is practically normal to the substrate (Fig 1a). The crystallite size and orientation depend weakly on substrate and ZnS concentration [10]. From Fig. 1, the crystallite size S can be calculated by [11]

$$S = \frac{K\lambda}{B \cos \theta} \quad (1)$$

where λ is the wavelength of the X-rays and θ the Bragg angle. K is known as the Scherrer constant and B the broadening of the diffraction line measured at half its maximum intensity. The crystallite sizes increase with film thickness.

The sputtering technique [12] for preparation of $(\text{Cd}_{1-x}\text{Zn}_x)\text{S}$ thin film solid solutions has revealed that for $x \geq 0.85$, the films have cubic structure, and for $x < 0.7$ the films have hexagonal structure. Fig. 2b shows the X-ray diffraction pattern for a powder sample of $(\text{Cd}_{1-x}\text{Zn}_x)\text{S}$ with $x = 0.41$. The pattern was indexed in terms of a hexagonal unit cell of $a = 0.402$ nm and $c = 0.653$ nm. These calculated parameters indicate small deviation from Vegard's law for such solid solutions. This deviation was previously confirmed by Vitrikhovskii *et al* [1, 3].

There are six factors affecting the relative intensity of the diffraction lines on a powder pattern: polarization, structure, multiplicity, Lorentz polarization, absorption and temperature. Then the relative intensity of the powder pattern lines was calculated from the equation

$$I = |F|^2 P \left(\frac{1 + \cos^2 2\theta}{\sin^2 \theta \cos \theta} \right) \quad (2)$$

where P is the multiplicity factor which is the number of planes having the same spacing and $(1 + \cos^2 2\theta)/\sin^2 \theta \cos \theta$ is the Lorentz polarization factor which decreases the intensity of reflection at intermediate angles compared to those in forward or backward directions. The intensity of a diffraction line is directly proportional to the irradiated volume of the specimen and inversely proportional to the camera radius, but these factors are again constant for all diffraction lines and may be neglected. Omission of the temperature and absorption factors means that Equation 2 is valid only for lines fairly close together on the pattern. If an exact expression is required, the absorption factor $A(\theta)$ and the temperature factor e^{-2M} must be inserted in Equation 2

$$I = |F|^2 P \left(\frac{1 + \cos^2 2\theta}{\sin^2 \theta \cos \theta} \right) A(\theta) e^{-2M} \quad (3)$$

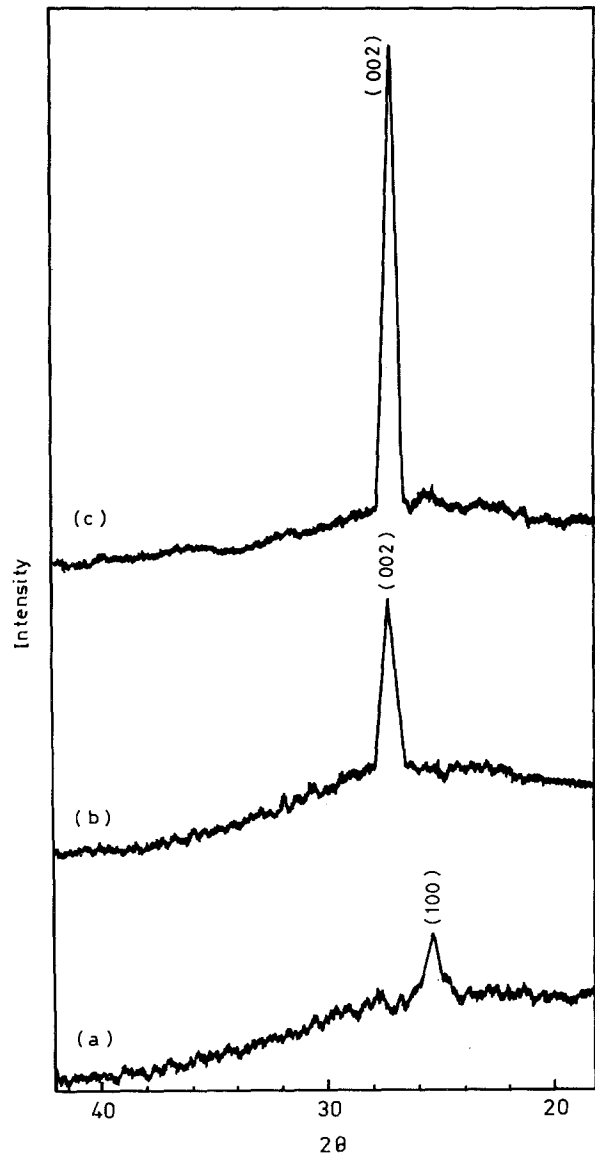


Figure 1 X-ray diffractogram of a freshly deposited $(\text{Cd}_{1-x}\text{Zn}_x)\text{S}$ film of (a) 273 nm thickness, (b) 200 nm thickness, with cobalt 0.00325%. (c) 70 nm thickness, with cobalt 0.0325%.

The effect of the thermal vibration on the scattering mechanism is ignored in the present calculation because it is very tedious to calculate it for such a solid solution. The absorption factor is also neglected in our calculation because it is independent of θ and so does not enter into the calculation of the relative intensities.

The structure factor F is related to the atomic scattering factor by the relation

$$F_{hkl} = \sum_{n=1}^N f_n \exp [2\pi i(hu_n + kv_n + lw_n)] \quad (4)$$

where the summation extends over all the N atoms of the unit cell. The atomic scattering factor of the solid solution $(\text{Cd}_{1-x}\text{Zn}_x)\text{S}$ atom is given by [13]

$$\begin{aligned} f_{av.} &= f_{\text{Cd}} + f_{\text{Zn}} \\ f_{av.} &= 0.59f_{\text{Cd}} + 0.41f_{\text{Zn}} \end{aligned}$$

where f_{Cd} and f_{Zn} are the atomic fractions of cadmium and zinc respectively.

For hexagonal $(\text{Cd Zn})\text{S}$, there are two molecules per unit cell, each molecule contains either a zinc or a cadmium atom joined to a sulphur atom located in the

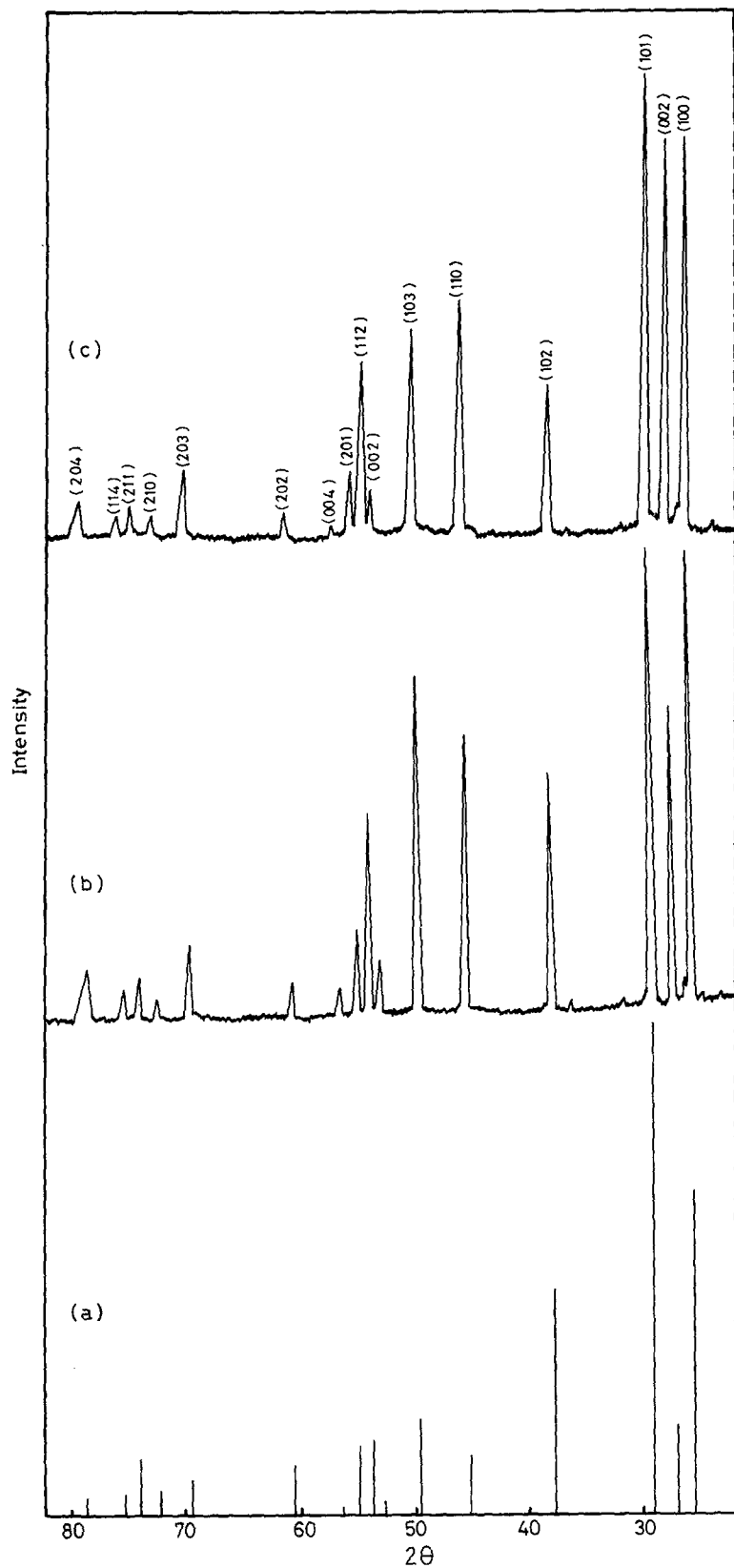


Figure 2 X-ray diffractogram of $(\text{Cd}_{1-x}\text{Zn}_x)\text{S}$ powder. (a) The theoretical calculation of the relative intensity. (b) $(\text{Cd}_{1-x}\text{Zn}_x)\text{S}$ which $x = 0.41$. (c) The effect of cobalt as a dopant in the matrix of $(\text{Cd}_{1-x}\text{Zn}_x)\text{S}$.

following positions
Zn or Cd:

$$000, \frac{1}{3}, \frac{2}{3}, \frac{1}{2},$$

and S:

$$00 \frac{3}{8}, \frac{1}{3}, \frac{2}{3}, \frac{7}{8}.$$

Equation 2 will be illustrated by the calculation of the position and relative intensities of the diffraction lines on a Debye-Scherrer pattern of $(\text{Cd}_{1-x}\text{Zn}_x)\text{S}$ made with $\text{CuK}\alpha$ radiation. The calculations are mostly shown in Fig. 2a.

A comparison of the calculated relative intensity of the planes with our experimental results shows a considerable difference. This could be attributed to the inhomogeneity of the distribution of cadmium and zinc atoms with the ratio of their atomic fraction in the solid solution. The planes of higher intensity may be enriched by cadmium atoms at the expense of zinc atoms as shown from the theoretical calculation because the atomic scattering factor of cadmium is about twice that of zinc. Accordingly the planes with lower relative intensity may be enriched by zinc atoms at the expense of cadmium atoms.

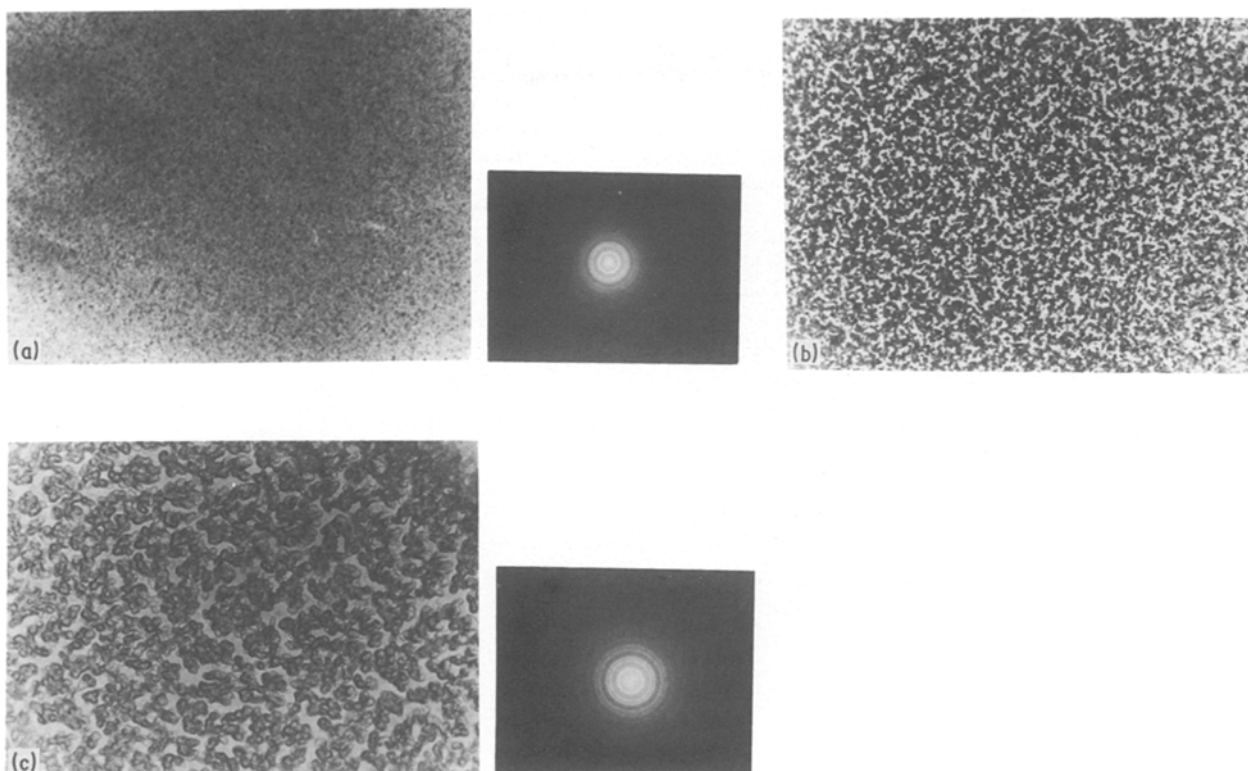


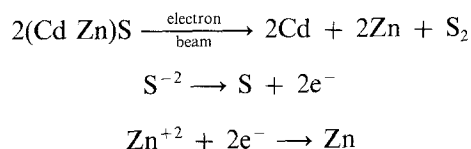
Figure 3 Transmission and diffraction electron micrographs for a freshly deposited $(\text{Cd}_{1-x}\text{Zn}_x)\text{S}$ film before and after decomposition. (a) Film before decomposition ($27\,000\times$). (b) The agglomeration of the layers under electron irradiation before decomposition ($27\,000\times$). (c) Film after decomposition at high electron beam intensities ($27\,000\times$).

Fig. 2c shows the effect of cobalt as a dopant in the matrix $(\text{Cd}_{1-x}\text{Zn}_x)\text{S}$. The change in the relative intensity is clear for (1 0 0), (0 0 2), (1 0 2), (1 1 0) and (1 0 3) planes. This change which increases for some planes and decreases for others indicates that the cobalt atoms replace either zinc or cadmium atoms in their regular sites in the lattice and do not fit in interstitial sites. Most probably, the cobalt ion ($r = 0.072\text{ nm}$) replaces either the zinc ion ($r = 0.074\text{ nm}$) or the cadmium ion ($r = 0.097\text{ nm}$). Since the atomic scattering factor of cobalt is approximately equal to that of zinc i.e. the replacement of a zinc ion by a cobalt ion does not practically affect the intensity of the planes.

When a solid is subjected to an investigation by electron microscope, it will certainly be affected by the electron beam. The produced effect differs from one substance to another depending on the type and nature of the specimen, its thermal conductivity, melting point, heat production and the environment. The effect also depends on the electron beam intensity which is very much influenced by the operating voltage and the vacuum conditions.

The electron beam has both ionizing and heating effects on the bombardment specimen. To explain the decomposition of $(\text{Cd Zn})\text{S}$ solid solution we should expect that both mechanisms participate. It may be suggested that a cadmium ion or zinc ion captures an electron from the electron beam forming a zinc or a cadmium atom and a sulphur ion becomes a sulphur atom with the secondary emission of an electron. The sulphur atoms react with each other to form sulphur molecules, which migrate through the specimen to the surface as sulphur gas. The decomposition of $(\text{Cd Zn})\text{S}$

may be represented according to the following reaction



Either of the two metal or sulphur atoms formed is unstable and when the conditions are satisfied an atom leaves its original occupied lattice site and wanders through the lattice by jumping to an interstitial position. However, the wandering atom may have its fate outside the original lattice and escape to the surface.

A sequence of the transmission electron micrographs, (Fig. 3) shows the various stages of $(\text{Cd Zn})\text{S}$ films deposited on amorphous substrate before and after decomposition. Fig. 3a shows that the thin film must be undertaken at low beam intensity to avoid decomposition by the electron beam. However, at high beam intensities $(\text{Cd Zn})\text{S}$ layers decompose leaving the grain boundaries decorated by metallic cadmium and zinc particles (Fig. 3c). Fig. 3b shows the agglomeration of the layers for the starting decomposition and the thermal effect of the electron beam.

The corresponding electron diffraction patterns for the specimen before and after exposure to bombardment by 80 KV electrons is shown in Fig. 3a, c. Analysis of the final diffraction patterns indicates the existence of both cadmium and zinc metal. Fig. 3c is taken as an indication that partial decomposition has occurred under electron bombardment.

References

1. N. I. VITRIKHOVSK and I. B. MIZETSKAYA, *Sov. Phys. Solid State*, **2** (1961) 2301.
2. F. KEFFRO and A. M. PORTIS, *J. Chem. Phys.* **27** (1957) 675.
3. P. DOMENS, M. CADENE, G. W. COHENSOLAL, S. MARTINUZZI and C. BROUTY, *Phys. Status Solidi a* **59** (1980) 201.
4. W. KANE, J. P. SPRATT, L. W. NERSHINGE and I. H. KHANE, *J. Electrochem. Soc.* **113** (1966) 136.
5. H. W. LEVERENZ, "An Introduction to the Luminescence of Solids" (Wiley, New York, 1950).
6. N. T. GORDON, F. SEITZ and F. J. QUINLAN, *Chem. Phys.* **7** (1939) 4.
7. Z. MORLIN and S. TERMMEL, *Czechoslovak J. Phys.* **3B** (1963) 216.
8. N. ARPIARIAN, *J. Chem. Phys.* **55** (1958) 667.
9. S. TOLOANSKY, "Introduction to Interferometry" 2nd Edn (Longmans, London, 1973) p. 157.
10. F. LEDAR and M. GINTER, Private communication, Montpellier (1978).
11. M. KAKUDO and N. KASAI, "X-ray Diffraction by Polymer" Kodansha Ltd (Elsevier Publishing Company, Amsterdam, 1972).
12. N. A. VLASENKO and N. K. KONOVELTS, *Ukr. Fiz. Zh* **14** (1969) 1578.
13. B. D. CULLITY, "Elements of X-ray Diffraction" 2nd Edn (Addison-Wesley, Reading, MA, 1978).

Received 10 December 1987

and accepted 29 April 1988